Cell, Vol. 102, 315–323, August 4, 2000, Copyright ©2000 by Cell Press

# Regulated Step in Cholesterol Feedback Localized to Budding of SCAP from ER Membranes

**Axel Nohturfft, Daisuke Yabe, Joseph L. Goldstein,* Michael S. Brown,* and Peter J. Espenshade**
Department of Molecular Genetics
University of Texas
Southwestern Medical Center
Dallas, Texas 75390

## Summary

**SREBPs exit the ER in a complex with SCAP. Together, they move to the Golgi where SREBP is cleaved, releasing a fragment that activates genes encoding lipid biosynthetic enzymes. Sterols block ER exit, preventing cleavage, decreasing transcription, and achieving feedback control of lipid synthesis. Here, we report an in vitro system to measure incorporation of SCAP into ER vesicles. When membranes were isolated from sterol-depleted cells, SCAP entered vesicles in a reaction requiring nucleoside triphosphates and cytosol. SCAP budding was diminished in membranes from sterol-treated cells. Kinetics of induction of budding in vitro matched kinetics of ER exit in living cells expressing GFP-SCAP. These data localize the sterol-regulated step to budding of SCAP from ER and provide a system for biochemical dissection.**

## Introduction

Cholesterol homeostasis in mammalian cells is controlled by a feedback regulatory system that senses the cholesterol content of membranes and appropriately modulates the transcription of genes required for cholesterol supply. The coordinate expression of these genes is orchestrated by a family of membrane-bound transcription factors called Sterol Regulatory Element Binding Proteins (SREBPs) (Brown and Goldstein, 1997, 1999).

Newly synthesized SREBPs are embedded in membranes of the ER and nuclear envelope in a hairpin orientation. SREBPs are comprised of three domains: (1) an $NH_2$-terminal domain of ~480 amino acids that faces the cytosol and functions as a transcription factor of the basic helix-loop-helix-leucine zipper family; (2) a membrane-anchoring domain of ~80 amino acids consisting of two membrane-spanning sequences that are separated by a hydrophilic loop of ~30 amino acids that projects into the lumen; and (3) a regulatory domain of ~590 amino acids that extends into the cytosol (Brown and Goldstein, 1997).

The activities of all three SREBP isoforms (SREBP-1a, -1c, and -2) are regulated by the cell's sterol content. In sterol-depleted cells, two sequential cleavages release the $NH_2$-terminal transcription factor domains of SREBPs from membranes (Brown and Goldstein, 1999). The first cleavage is catalyzed by a membrane-bound serine protease, designated Site-1 protease (S1P), that clips SREBPs at a leucine–serine bond within the luminal loop that links the two transmembrane domains (Duncan et al., 1997). This cleavage generates the substrate for a second enzyme, a membrane-bound zinc metalloprotease, designated Site-2 protease (S2P), that cleaves the $NH_2$-terminal fragment of each SREBP at a point that is three amino acids into the first transmembrane domain (Rawson et al., 1997; Duncan et al., 1998). The released $NH_2$-terminal fragment migrates to the nucleus where it activates transcription of the LDL receptor gene and more than 20 genes involved in lipid biosynthesis (Brown and Goldstein, 1997; Edwards and Ericsson, 1999). When cholesterol levels rise in cells, SREBPs are no longer cleaved by S1P. As a result, cholesterol synthesis and uptake of LDL decrease, thereby maintaining cholesterol homeostasis in a classic feedback fashion (Brown and Goldstein, 1997).

Cleavage of SREBPs by S1P requires the action of SREBP Cleavage-Activating Protein (SCAP), a polytopic membrane protein of 1276 amino acids (Hua et al., 1996a). SCAP is divided broadly into two domains (Nohturfft et al., 1998a). The $NH_2$-terminal 730 amino acids are thought to form eight membrane-spanning segments with three N-linked oligosaccharide chains attached to the luminal loops. The COOH-terminal 546 amino acids project into the cytosol and contain five copies of a protein/protein interaction motif called the WD repeat. The WD repeat domain of SCAP binds to the COOH-terminal regulatory domain of SREBP, forming a complex that is required for SREBP cleavage by S1P (Sakai et al., 1997, 1998). Complex formation is also essential to stabilize the SREBP precursor. In mutant cells that lack SCAP, the levels of all SREBP precursors are reduced, apparently as a result of premature degradation, and there is also no cleavage by S1P (Rawson et al., 1999).

A clue to the role of SCAP emerged from the observation that the uncleaved precursor forms of SREBPs are found in the ER (Wang et al., 1994; Duncan et al., 1997), whereas the active form of S1P is located in a post-ER compartment (DeBose-Boyd et al., 1999; Espenshade et al., 1999). Cleavage of SREBPs thus requires that the SREBPs be transported from the ER to the post-ER compartment, most likely the Golgi. This conclusion is supported by experiments in which S1P was artificially induced to relocate from the Golgi to the ER. Under those conditions, the SREBPs were cleaved by S1P in a reaction that no longer required SCAP and was no longer inhibited by sterols (DeBose-Boyd et al., 1999).

Biochemical and genetic evidence has led to a model in which SCAP carries SREBPs from the ER to the Golgi and cholesterol blocks this transport. This model is supported by analysis of the N-linked oligosaccharides of SCAP. In cells replete with cholesterol, the N-linked oligosaccharide chains on SCAP are sensitive to hydrolysis by endoglycosidase H (endo H), indicating that SCAP is located in the ER. Upon sterol depletion, the oligosaccharide chains on SCAP become resistant to endo H as a consequence of modification by Golgi-specific enzymes (Nohturfft et al., 1998b, 1999). Cholesterol modulates

*To whom correspondence should be addressed (e-mail: jgolds@mednet.swmed.edu [J. L. G.], mbrow1@mednet.swmed.edu [M. S. B.]).

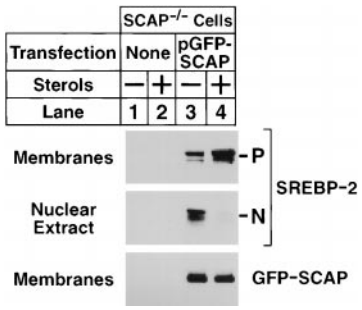


Figure 1. GFP-SCAP Restores Sterol-Regulated Cleavage of SREBP-2 in SCAP-Deficient Hamster Cells

On day 0, SCAP-deficient SRD-13A cells (lanes 1 and 2) and SRD-13A cells stably transfected with pGFP-SCAP (CHO/pGFP-SCAP cells) (lanes 3 and 4) were set up at a density of $4 \times 10^5$ cells per 60 mm dish in medium A supplemented with 5% FCS. On day 1, cells were switched to medium A supplemented with 5% newborn calf lipoprotein-deficient serum and 1% (w/v) HPCD in the absence or presence of sterols (10 μg/ml 25-HC plus 10 μg/ml cholesterol in 0.2% (v/v) ethanol). After incubation for 2 hr at 37°C, cells were harvested, and membrane and nuclear extract fractions were prepared as described (DeBose-Boyd et al., 1999). Aliquots of membranes (9 μg and 2 μg for SREBP-2 and SCAP blots, respectively) and nuclear extracts (15 μg) were subjected to 8% SDS-PAGE and immunoblotted with antibodies to SREBP-2 (IgG-7D4) or SCAP (IgG-R139). P and N denote the precursor and nuclear forms of SREBP-2, respectively.

this ER-to-Golgi transport of SCAP by interacting, directly or indirectly, with an ~170 amino acid segment within the polytopic membrane attachment domain of SCAP that has been termed the sterol-sensing domain. Domains with similar sequences have been identified in several membrane proteins whose actions are related to cholesterol (Brown and Goldstein, 1999).

In the current study, we use a green fluorescent protein (GFP)-SCAP fusion protein to visualize the transport of SCAP from the ER to the Golgi in sterol-deprived cells. We then establish an in vitro system to measure the incorporation of SCAP into ER-derived membrane vesicles. Using this assay, we show that sterol deprivation of intact cells renders the ER membrane competent to discharge SCAP into budding vesicles in vitro and that the time course for the acquisition of this competence matches the time course for the exit of GFP-SCAP from the ER in vivo.

## Results

### Visualizing ER-to-Golgi Transport of SCAP in Living Cells

To study the transport of SCAP from ER to Golgi in living cells, we constructed a chimeric cDNA encoding the green fluorescent protein (GFP) attached to the $NH_2$ terminus of hamster SCAP, thereby orienting the GFP domain toward the cytoplasmic face of the membrane. The biological activity of this GFP-SCAP fusion protein was assessed by stably transfecting the GFP-SCAP cDNA into mutant CHO cells (designated SRD-13A) that lack SCAP activity. SRD-13A cells express no detectable SCAP mRNA or protein, which leads to markedly reduced levels of the precursor as well as the nuclear forms of SREBP (Rawson et al., 1999). Figure 1 shows an immunoblot analysis of endogenous SREBP-2 and its proteolytic processing in nontransfected SRD-13A cells (lanes 1 and 2) and in SRD-13A cells that had been stably transfected with the GFP-SCAP cDNA (lanes 3 and 4). GFP-SCAP raised the level of the SREBP-2 precursor in membranes and permitted the generation of the cleaved nuclear fragment in a sterol-regulated fashion.

Figure 2 shows an experiment in which we used confocal microscopy to examine the subcellular localization of GFP-SCAP in the stably transfected SRD-13A cells. When the GFP-SCAP cells were cultured in medium containing fetal calf serum (FCS) as a source of sterols, GFP-SCAP displayed a diffuse, reticular pattern corresponding to the ER (panel A). Antibodies to Golgi α-mannosidase II (panel B) stained a structure that showed little overlap with GFP-SCAP under these conditions (panel C). To deplete the cells of sterols, we incubated the cells for 5 hr in medium containing 1% hydroxypropyl-β-cyclodextrin (HPCD), an agent that is known to remove sterols from intact cells (Kilsdonk et al., 1995). After this treatment, GFP-SCAP showed strong juxtanuclear staining in addition to the reticular ER pattern (panel D). Colocalization of GFP-SCAP with Golgi α-mannosidase II (panel E) confirmed the localization of GFP-SCAP in or near the Golgi (panel F). In contrast, when cells were incubated with HPCD in the presence of sterols, GFP-SCAP remained localized to the ER (panels G–I). The signal for GFP-SCAP was specific inasmuch as nontransfected SRD-13A cells showed no detectable fluorescence under similar conditions (data not shown). These data indicate that GFP-SCAP moves to the Golgi region in sterol-depleted, but not sterol-overloaded cells.

To study the movement of GFP-SCAP from the ER to the Golgi in more detail, we used time-lapse confocal microscopy of living cells to follow the movement of GFP-SCAP upon removal of sterols (Figure 3). To begin the experiment, cells were cultured in FCS and then switched to medium containing HPCD in the absence of sterols. At $t = 0$ min, GFP-SCAP was localized to the ER in a diffuse, reticular pattern. As early as 15 min after addition of HPCD, GFP-SCAP was seen in vesicular structures that originated from peripheral sites in the ER and appeared to migrate toward the Golgi. These structures resembled the transport intermediates observed during the movement of GFP-tagged vesicular stomatitis virus glycoprotein (VSVG) from the ER to Golgi in living cells (Presley et al., 1997). As shown in Figure 3, by 30 min we observed obvious accumulation of GFP-SCAP in the Golgi region. In the time-lapse micrographs, we observed that transport intermediates continued to form, and GFP-SCAP became increasingly concentrated in the Golgi region over the 2.5 hr. The time-lapse movie can be viewed at http://www.cell.com/cgi/content/full/102/3/315/DC1.

### Reconstituting ER Export of SCAP In Vitro

Transport of proteins from the ER to the Golgi is initiated by the incorporation of cargo proteins into transport vesicles that bud from the ER and subsequently fuse with cis elements of the Golgi (Palade, 1975). In important experiments, Rexach et al. (1991) and Rowe et al. (1996) established systems in which the formation of ER-derived transport vesicles can be reconstituted in vitro by incubating microsomes in the presence of nucleoside triphosphates (ATP/GTP) and cytosol. Vesicles formed during this reaction are found in the supernatant after centrifugation at 16,000 × g, whereas the donor membranes are found in the pellet (Rexach and Schekman, 1991; Rowe et al., 1996). We used the methods

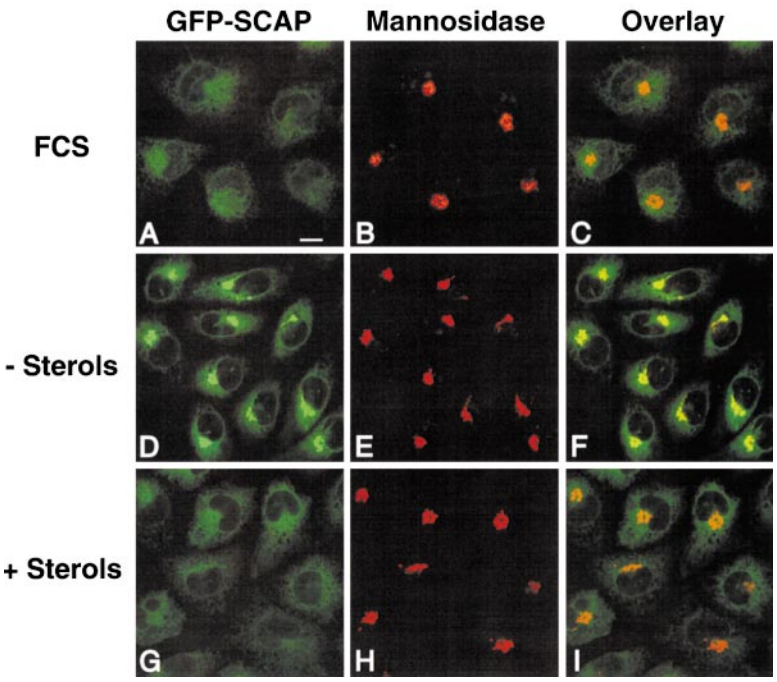


Figure 2. Visualization of Sterol-Regulated ER-to-Golgi Transport of GFP-SCAP in Hamster Cells

Stably transfected CHO/pGFP-SCAP cells were set up as described in Experimental Procedures in medium A containing 5% FCS. On day 2, cells were switched to medium A supplemented with 5% lipoprotein-deficient serum and 1% HPCD in the absence or presence of sterols (10 μg/ml 25-HC and 10 μg/ml cholesterol in 0.2% ethanol). After 5 hr at 37°C, cells were fixed and stained with antibody as previously described (Sakai et al., 1997) except that 0.5% (v/v) Triton X-100 was used for cell permeabilization. Antiserum against Golgi α-mannosidase II (1:1000 dilution) was visualized with 15 μg/ml goat anti-rabbit IgG conjugated to Alexa 594 (Molecular Probes). Cells were imaged for GFP-SCAP (A, D, and G) or α-mannosidase II (B, E, and H) using a confocal microscope (Sakai et al., 1997). Panels (C), (F), and (I) are merged images of GFP-SCAP and Golgi α-mannosidase II. Bar, 10 μm.

established by these laboratories to study the incorporation of SCAP into ER-derived vesicles in vitro.

Figure 4 shows the basic features of the in vitro vesicle-formation assay. CHO-K1 cells were grown in the presence of lipoprotein-deficient serum and HPCD to deplete the cells of cholesterol. Microsomes were isolated from these cells by centrifugation and incubated under conditions that permit budding of vesicles. The resulting vesicle and membrane fractions were separated by centrifugation and analyzed for the presence of SCAP and other proteins by SDS-PAGE and immunoblotting. Incubation of microsomes in the presence of cytosol and nucleoside triphosphates (ATP, GTP, and an ATP-regenerating system) at 37°C led to the time-dependent appearance of SCAP in the vesicle fraction (top panel of Figure 4, lanes 4–8). When ATP/GTP or cytosol was omitted from the reaction mixture or when the reaction was incubated on ice, no SCAP was found in the vesicle fraction (lanes 1–3), and all of the SCAP remained in the donor membranes (lanes 9–11). For comparison, we also blotted with an antibody against p58, a type I membrane protein that cycles between ER and post-ER compartments (Klumperman et al., 1998) and has been previously used as a marker to study ER export in vitro (Rowe et al., 1996). As shown in the second panel of Figure 4, p58 was released into the vesicle fraction. This reaction also required ATP/GTP, cytosol, and temperature (compare lanes 1–3 with lane 8). The efficiency of SCAP budding in Figure 4, as determined by scanning the immunoblot and quantifying it by densitometry, was 27% at 15 min as compared to 20% for p58. In the seven other experiments described below, the efficiency of SCAP budding ranged from 11% to 63% with a mean of 27%.

To exclude the possibility that the vesicle fraction was created by nonspecific fragmentation of the donor membranes, the fractions were analyzed with antibodies against the ER-resident proteins grp94, grp78 (BiP), and

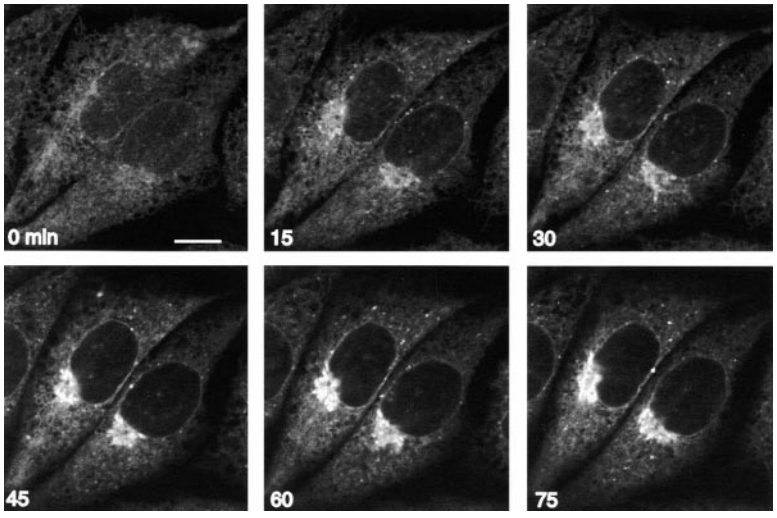


Figure 3. Visualization of Transport of GFP-SCAP from ER-to-Golgi in Living Hamster Cells

On day 0, stably transfected CHO/pGFP-SCAP cells were set up in medium A supplemented with 5% FCS. On day 2 at t = 0 hr, cells were switched to medium A supplemented with 5% lipoprotein-deficient serum and 1% HPCD in the absence of sterols. Cells were maintained at 37°C in 5% $CO_2$, and images were collected every 2.5 min for 2.5 hr using a confocal microscope with an open pinhole. Bar, 10 μm. A QuickTime movie sequence of these events is available at http://www.cell.com/cgi/content/full/102/3/315DC1.

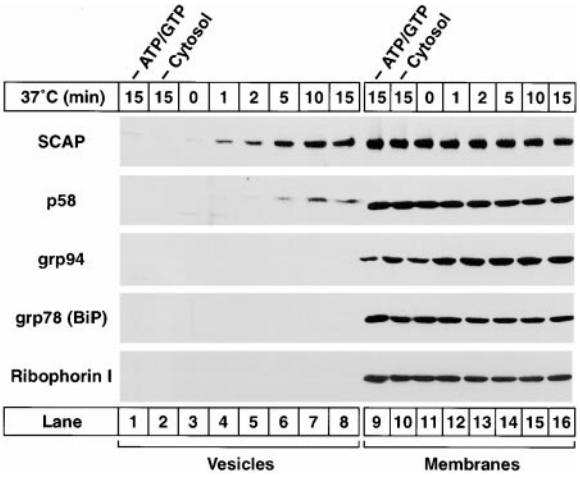


Figure 4. SCAP from Cholesterol-Depleted Hamster Cells Is Incorporated into Vesicles In Vitro

On day 0, CHO-K1 cells were set up at $8 \times 10^5$ cells per 10 cm dish in medium A containing 5% FCS. On day 2, cells were switched to medium A containing 5% lipoprotein-deficient serum and 1% HPCD, incubated for 2 hr at 37°C, and harvested. Microsomes were prepared and incubated in vitro at 37°C for the indicated time in the presence of cytosol, ATP, GTP, and an ATP-regenerating system as described in Experimental Procedures. The mixtures were centrifuged to separate vesicle and membrane fractions that were subjected to SDS-PAGE and immunoblotted with IgG-R139 (anti-SCAP), anti-p58, anti-KDEL (grp94 and grp78), and anti-ribophorin I as indicated.

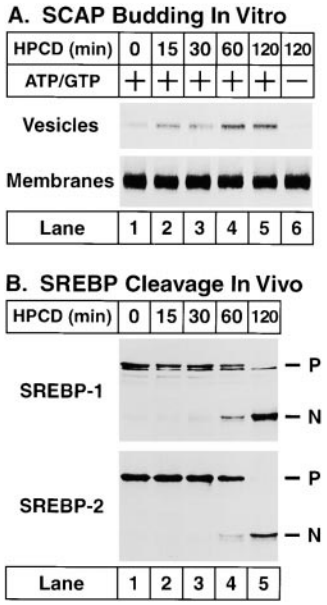


Figure 5. Induction of SCAP Budding In Vitro and SREBP Cleavage In Vivo upon Treatment of Hamster Cells with HPCD

On day 0, CHO-K1 cells were set up as described in Figure 4. On day 2, cells were refed with medium A containing 5% lipoprotein-deficient serum, 10 μg/ml cholesterol, 1 μg/ml 25-HC, 0.5% ethanol, and incubated for 3 hr at 37°C. The cells were then deprived of sterols by switching to medium A containing 5% lipoprotein-deficient serum, 1% HPCD, and 0.5% ethanol for the indicated time. Cells were fed with the HPCD-containing medium in a staggered fashion such that they were all harvested at the same time at 120 min. All cells received 25 μg/ml ALLN added in 0.1% DMSO during the last 120 min.

(A) Microsomes were prepared and used in an in vitro vesicle-formation assay as described in Figure 4. The resulting vesicle and membrane fractions were subjected to SDS-PAGE and immunoblotted with IgG-R139 (anti-SCAP).

(B) Total cell extracts were prepared by lysing washed cell monolayers with 200 μl of Buffer C, after which the lysates from duplicate dishes were pooled and sheared through a 25-gauge needle. Aliquots (100 μg protein) were subjected to 8% SDS-PAGE and immunoblotted with IgG-2A4 (top) and IgG-7D4 (bottom), respectively. P and N denote the precursor and nuclear mature forms of SREBPs, respectively.

ribophorin I. All three proteins remained confined to the donor membranes (lanes 9–16), and none were visualized in the vesicle fraction (lanes 1–8). Taken together, the results of Figure 4 show that the incorporation of SCAP into vesicles in vitro constitutes a specific sorting event that is dependent on nucleoside triphosphates, cytosol, and temperature.

### Sterol Regulation of SCAP Budding

The next set of experiments was designed to determine whether incorporation of SCAP into vesicles is suppressed when cells have been loaded with sterols. In Figure 5A, CHO-K1 cells were initially grown in the presence of cholesterol and 25-hydroxycholesterol (25-HC), which causes SCAP to be retained in the ER (see Figures 2 and 3) (Nohturfft et al., 1998b, 1999). Subsequently, cells were switched for increasing periods of time to medium containing HPCD. Microsomes from these cells were then subjected to an in vitro vesicle-formation assay. When cells had been continually grown in the presence of sterols, very little SCAP was found in the vesicle fraction (Figure 5A, lane 1), and most of the protein remained in the membrane fraction. The amount of SCAP released into vesicles increased significantly after the cells had been incubated in sterol-depleting medium for only 15 min, and it reached a maximum after 1 hr of such preincubation (lanes 2–5). Release of SCAP into the vesicle fraction did not occur when ATP and GTP were omitted from the reaction (lane 6).

To compare the induction of SCAP budding with the kinetics of SREBP cleavage, total cell extracts from the same cells used in Figure 5A were immunoblotted with antibodies against SREBP-1 and SREBP-2 (Figure 5B). Shifting cells from sterol-containing to sterol-depleting medium led to the appearance of the nuclear mature form of both SREBPs after 60 min (lane 4). After 120 min, the precursor forms of SREBP-1 and SREBP-2 had disappeared, and only the nuclear form was seen (lane 5).

Figure 6A shows an experiment in which CHO-K1 cells were first depleted of sterols and then switched to sterol-containing medium for increasing periods of time. Microsomes from these cells were then used in a vesicle budding assay. In samples from cells grown without sterols, SCAP was found in the vesicle fraction (lane 4), and this effect was dependent on nucleoside triphosphates, cytosol, and temperature (lanes 1–3). When the cells were preincubated with sterols for as little as 0.5 hr, there was a detectable decrease in SCAP budding and inhibition was virtually complete after a 2 hr incubation (lanes 5–8).

To address the specificity of the sterol-mediated inhibition of SCAP budding, we analyzed the effect of sterol preincubation on the budding of other proteins that are known to enter ER-derived transport vesicles. The most

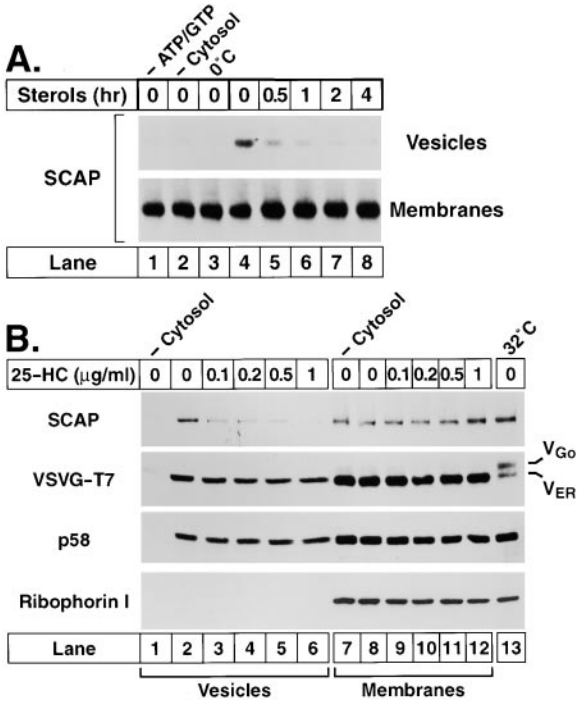


Figure 6. Loss of SCAP Budding in Membranes from Sterol-Treated Hamster Cells

(A) On day 0, CHO-K1 cells were set up as described in Figure 4. On day 2, the cells were switched to medium A containing 5% lipoprotein-deficient serum, 50 μM compactin (an inhibitor of cholesterol synthesis), 50 μM sodium mevalonate, 0.5% ethanol, and 1% HPCD and incubated at 37°C for 1 hr. The cells were then incubated for the indicated time with medium A containing 5% lipoprotein-deficient serum, 50 μM compactin, 50 μM sodium mevalonate, and 0.5% ethanol in the absence or presence of sterols (1 μg/ml 25-HC plus 10 μg/ml cholesterol). Additions of sterols were made in a staggered fashion such that all samples were harvested at the same time. Microsomes were prepared and analyzed in the in vitro vesicle-formation assay for 15 min at 37°C as described in Figure 4. Vesicle and membrane fractions were analyzed by SDS-PAGE and immunoblotted with IgG-R139 (anti-SCAP). (B) On day 0, CHO/VSVG-T7 cells were set up in medium A containing 5% FCS and cultured at 40°C. On day 2, cells were refed with medium A containing 5% lipoprotein-deficient serum, 50 μM compactin, 50 μM sodium mevalonate, 0.5% ethanol, and 1% HPCD, and incubated at 40°C for 1 hr. Cells were then washed twice with PBS and refed with medium A containing 5% lipoprotein-deficient serum, 50 μM compactin, 50 μM sodium mevalonate, and 0.5% ethanol in the absence or presence of the indicated concentration of 25-HC, and incubated at 40°C for 3 hr (lanes 1–12). A replicate set of cells were cultured at 40°C in medium A containing 5% FCS, but then transferred to 32°C (without change of medium) for the last 4 hr (lane 13). All cells were harvested at the same time, and microsome fractions were incubated for 15 min in the standard in vitro vesicle-formation assay as described in Figure 4, except that the cells were not frozen prior to preparation of microsomes and the temperature of the budding reaction was 32°C rather than 37°C. Vesicle (lanes 1–6) and membrane (lanes 7–13) fractions were subjected to SDS-PAGE and immunoblotted with IgG-R139 (anti-SCAP), anti-T7•Tag (VSVG-T7), anti-p58, and anti-ribophorin I. $V_{GO}$ and $V_{ER}$ denote the Golgi-modified and ER forms of VSVG-T7, respectively.

widely-studied of these proteins is vesicular stomatitis virus glycoprotein (VSVG), the envelope glycoprotein from the temperature-sensitive strain tsO45. At 40°C, VSVG/tsO45 misfolds and accumulates in the ER. Upon shifting to 32°C, the protein refolds, and it is released from the ER and transported to the Golgi and then to the plasma membrane (Beckers et al., 1987; Bergmann, 1989). We generated a CHO-K1 cell line stably expressing a fusion protein consisting of VSVG/tsO45 with a COOH-terminal T7 epitope tag (VSVG-T7). In control experiments, we verified that the N-linked oligosaccharides of VSVG-T7 remained in an endo H–sensitive configuration when cells were grown at 40°C, indicating that the protein was retained in the ER. Upon temperature shift from 40°C to 32°C, the protein became endo H resistant and ran more slowly on SDS-PAGE, owing to sialylation in the Golgi (Bergmann, 1989).

In Figure 6B, cells were cultured with different concentrations of 25-HC at 40°C. Membranes were isolated and incubated at 32°C to permit budding of VSVG-T7 in vitro. Vesicles and membrane fractions were blotted with antibodies against SCAP and VSVG-T7 as well as p58 and ribophorin I. As expected, increasing concentrations of 25-HC in the culture medium caused SCAP to be excluded from budding vesicles (lanes 3–6). In contrast, budding of both VSVG-T7 and p58 was unaffected by 25-HC. To demonstrate that the VSVG-T7 at 40°C resided in ER membranes, we incubated some of the culture dishes at 32°C. Under these conditions some of the VSVG-T7 moved to the Golgi where it was modified by Golgi-resident sialyltransferases and hence the protein migrated more slowly than the protein isolated from cells grown at 40°C (lane 13). As a negative control, we blotted with an antibody against the ER-resident protein ribophorin I. None of this protein was seen in the vesicle fraction. We interpret the results of Figures 5 and 6 to indicate that sterols inhibit export of SCAP from the ER by specifically blocking its incorporation into transport vesicles.

Figure 7 shows an experiment in which the sterol specificity for the inhibition of SCAP budding was examined. CHO-K1 cells were incubated with increasing concentrations of different sterols, after which microsomes were prepared and used in the standard in vitro vesicle-formation assay. Incubation of cells with 25-hydroxycholesterol at a concentration as low as 0.1 μg/ml led to a marked decrease in SCAP budding (Figure 7A, lane 6; and Figure 7B, lane 3). 20-Hydroxycholesterol was the second most potent sterol with complete inhibition of budding at 1 μg/ml, followed by 7-ketocholesterol with complete inhibition at 10 μg/ml. Cholesterol and progesterone had no significant effect at concentrations up to 10 μg/ml. The lack of effect of cholesterol is attributable to inefficient cellular uptake from ethanol solutions (Krieger et al., 1978). This order of potency precisely matches that previously observed for sterol-mediated suppression of SREBP-1 cleavage in HeLa cells (Wang et al., 1994).

### Budding of SREBP Dependent on SCAP

If the in vitro membrane budding assay reflects the physiologic transport that occurs in vivo, then SREBPs should be incorporated into budding vesicles only when SCAP is present. To test this prediction, we transfected SCAP-deficient SRD-13A cells with plasmids encoding HSV-tagged SREBP-1a with or without SCAP. Cells were depleted of sterols for 2 hr, after which microsomes were prepared and subjected to an in vitro vesicle-formation assay. In cells that lacked SCAP, the vesicles contained a small amount of SREBP-1a (lane 2). Coexpression of

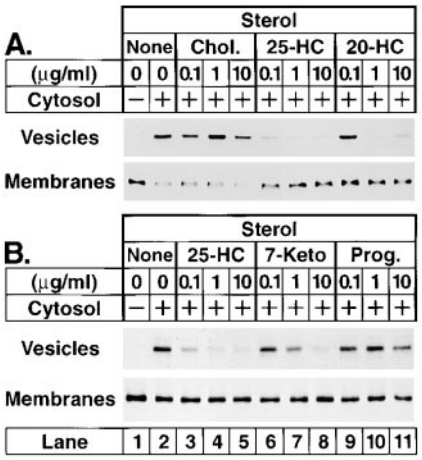


Figure 7. Sterol Specificity of Inhibition of SCAP Budding in Hamster Cell Membranes

On day 0, CHO-K1 cells were set up as described in Figure 4. On day 2, cells were switched to medium A containing 5% lipoprotein-deficient serum, 50 μM compactin, 50 μM sodium mevalonate, 0.5% ethanol, and 1% HPCD and incubated at 37°C for 1 hr. The cells were refed with medium A containing 5% lipoprotein-deficient serum, 50 μM compactin, 50 μM sodium mevalonate, 0.5% ethanol, and the indicated concentrations of cholesterol (Chol.), 25-HC, 20-hydroxycholesterol (20-HC), 7-ketocholesterol (7-Keto), or progesterone (Prog.). Cells were then incubated at 37°C for 3 hr and harvested. Microsomes were prepared and used in an in vitro vesicle-formation assay as described in Figure 4. The resulting vesicle and membrane fractions were subjected to SDS-PAGE and immunoblotted with IgG-R139 (anti-SCAP).

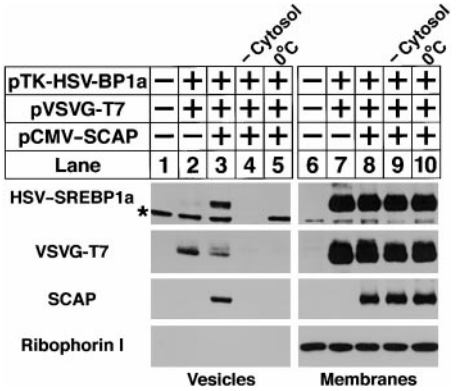


Figure 8. In Vitro Budding of SREBP Requires SCAP

On day 0, SRD-13A cells were set up at $6 \times 10^5$ cells per 10 cm dish as described in Experimental Procedures. On day 2, plasmid encoding HSV-tagged SREBP-1a (3 μg/dish, lanes 2 and 7; 1 μg/dish, lanes 3–5 and 8–10) (Hua et al., 1996b) was cotransfected with pCMV-SCAP (1 μg/dish; lanes 3–5 and 8–10) (Sakai et al., 1997) or pVSVG-T7 (0.5 μg/dish; lanes 2–5 and 7–10) as indicated. The plasmid pVAI, which increases protein expression from cotransfected cDNAs (Akusjarvi et al., 1987), was used to normalize the amount of HSV-SREBP-1a in the absence of the stabilizing SCAP protein (1 μg/dish, lanes 1–2 and 6–7). Total amount of DNA was adjusted to 5.5 μg/dish by addition of pTK and pcDNA3 empty vectors. Transfection was performed for 20 hr in medium A containing 5% FCS as described (DeBose-Boyd et al., 1999). On day 3, cells were depleted of sterols as in Figure 4. Microsomes were prepared and used in the in vitro vesicle-formation assay as described in Experimental Procedures with the following modifications: Buffers E and F contained 1.5 and 0.5 mM $Mg(OAc)_2$, respectively, and the reactions were performed at 28°C for 15 min in the standard buffer containing 1.5 mM rather than 2.5 mM $Mg(OAc)_2$. Vesicles (lanes 1–5) and membrane (lanes 6–10) fractions were subjected to SDS-PAGE and immunoblotted with anti-HSV•Tag (SREBP-1a), IgG-R139 (anti-SCAP), anti-T7•Tag (VSVG-T7), and anti-ribophorin I. Asterisk (*) denotes a cytosolic protein that crossreacts with anti-HSV•Tag antibody.

SCAP increased incorporation of SREBP-1a into vesicles by 9-fold (lane 3). SCAP-dependent budding of SREBP-1a required cytosol and temperature (lanes 4 and 5). Coexpression of SCAP did not increase the budding of co-transfected VSVG-T7 (compare lanes 2 and 3).

## Discussion

The current experiments, conducted in vivo and in vitro, provide strong support for the conclusion that sterols block the proteolytic processing of SREBPs by inhibiting the incorporation of SCAP into ER-derived vesicles that carry the SCAP/SREBP complex to the Site-1 protease. The experiments also provide a new system that should permit a dissection of the biochemical mechanism for this regulation. In the in vivo experiments, GFP-SCAP was observed to exit the ER within 30 min after cellular sterols were depleted by treatment with HPCD (Figure 3). In the in vitro experiments, the budding of SCAP into ER-derived vesicles was increased when the membranes were isolated after 15–30 min of cellular sterol depletion (Figure 5). This correlation helps to validate the in vitro assay as a true measure of the physiologically regulated budding process. The data also indicate that sterol depletion alters the properties of SCAP in the ER membrane in a fashion that persists when the membranes form vesicles in vitro.

After leaving the ER in sterol-depleted cells, the GFP-SCAP fusion protein followed a route that was similar to the route previously described for the movement of GFP-tagged VSVG protein (Presley et al., 1997). GFP-SCAP was observed to concentrate in vesicles that formed in the cell periphery and migrated to the Golgi region. The colocalization of GFP-SCAP fluorescence and α-mannosidase II immunofluorescence indicates that GFP-SCAP reached the region of the Golgi complex. However, the resolution of the confocal microscope is insufficient to determine whether GFP-SCAP actually entered the Golgi stacks or whether it remained in Golgi-associated intermediate compartments.

The experiments with GFP-SCAP must be interpreted in light of the fact that the amount of GFP-SCAP in the permanently transfected cells was at least 10-fold higher than the amount of SCAP in wild-type CHO cells as estimated by immunoblotting (data not shown). Despite the overabundance of GFP-SCAP in the transfected cells, SREBP processing was regulated normally by sterols (Figure 1), indicating that the overexpressed GFP-SCAP was interacting with SREBP and exiting the ER in a normal sterol-controlled manner. The proportion of GFP-SCAP that exited the ER and the proportion that recycled back to the ER before or after reaching the Golgi complex cannot be determined from these studies. Previous experiments suggest that SCAP recycles to the ER from the S1P-containing Golgi compartment (Nohturfft et al., 1999).

After cells were depleted of sterols, there was a close correspondence between the time required to visualize GFP-SCAP movement to the Golgi in vivo (Figure 3) and

the time required to detect increased SCAP budding from membranes in vitro (Figure 5A). Budding was diminished when membranes were prepared either from cells that were treated with increasing amounts of exogenously added sterols (Figures 6 and 7) or from cells that overproduced endogenous cholesterol as a result of an SREBP truncation (unpublished observations). The sterol specificity for suppression of SCAP budding in vitro (Figure 7) matched the known sterol specificity for the regulation of SREBP processing and cholesterol synthesis in vivo (Wang et al., 1994). Moreover, in vitro budding was not suppressed completely by sterols in cells that expressed mutants of SCAP that are known to be sterol resistant (unpublished observations). All of these observations support the assertion that the in vitro assay measured the physiologically relevant budding process.

In order to observe SCAP budding in vitro, it is necessary first to deplete the cells of sterols. Under these conditions, nearly all of the SREBP precursor disappears because it is processed to the mature form. Therefore, most of the SCAP in the budding vesicles is not likely to be associated with SREBPs. To demonstrate the SCAP dependence of SREBP-budding in vitro, we used membranes prepared from SRD-13A cells that lack endogenous SCAP. Inasmuch as these cells have low levels of SREBP precursors (Rawson et al., 1999), it was necessary to perform a transfection with a cDNA encoding SREBP-1a (Figure 8). Under these conditions, cotransfection of a cDNA encoding SCAP led to a major increase in SREBP budding in vitro. This SCAP dependence in vitro mirrors the SCAP dependence of SREBP cleavage in vivo (Rawson et al., 1999), providing further evidence for the physiologic relevance of the in vitro budding assay.

The sterol-regulated exit of SCAP from the ER appears to represent the first observed example of an ER exit process that is under metabolic control. Metabolic control differs from the quality-control process by which proteins are retained in the ER until they have undergone proper folding or posttranslational modification (Ellgaard et al., 1999). In the case of SCAP, ER retention is a central event in a physiologically regulated process.

The data from the in vitro assay establish that sterol depletion alters SCAP in the ER membrane as opposed to altering a cytosolic factor. In the budding assays, we used a constant preparation of cytosol obtained from livers of rats that were not deprived of cholesterol. The difference in the budding activity of ER membranes from sterol-depleted and sterol-overloaded cells must have been caused by an alteration in SCAP or in some other component of the membranes.

The mechanism by which SCAP is retained in the ER of sterol-replete cells is unknown. One possibility is that SCAP binds directly to sterols, thereby inducing a conformational change that abrogates its interaction with the cytosolic COPII budding machinery, which controls incorporation of cargo into ER vesicles (Springer et al., 1999). Another model, perhaps more likely, postulates that SCAP binds to a resident protein that holds it in the ER in the presence of sterols. When sterols are depleted, SCAP dissociates from this protein, and it is thereby free to enter budding vesicles. Whether these vesicles are the same as the ones that carry VSVG protein and other cargo, or whether SCAP enters a distinct population of vesicles, is currently unknown. It is clear, however, that SCAP entry into budding vesicles can be suppressed selectively under conditions in which the general process of vesicle budding is unaffected (Figure 6B).

## Experimental Procedures

### Materials

We obtained rabbit muscle creatine kinase and the sodium salts of ATP, GTP, and creatine phosphate from Boehringer; cholesterol from Alltech; 25-HC from Steraloids; *N*-acetyl-leucinal-leucinal-norleucinal (ALLN) and hexyl-β-D-glucopyranoside from Calbiochem; HPCD from Cyclodextrin Technologies Development (Gainesville, FL); monoclonal anti-KDEL antibody (IgG fraction) from StressGen (Victoria, Canada); monoclonal anti-T7•Tag antibody and anti-HSV•Tag antibody from Novagen; and horseradish peroxidase-conjugated, affinity-purified donkey anti-mouse and anti-rabbit IgG from Jackson ImmunoResearch. Polyclonal antibody IgG-R139 raised against hamster SCAP (amino acids 54–277 and 540–707) (Sakai et al., 1997), monoclonal antibody IgG-2A4 against human SREBP-1a (amino acids 301–407) (Sato et al., 1994), and monoclonal antibody IgG-7D4 against hamster SREBP-2 (amino acids 32–250) (Yang et al., 1995) have been described in the indicated references. Other polyclonal antibodies used in this study were generous gifts from the following laboratories: K. Moremen, University of Georgia, Athens, GA (anti-rat Golgi α-mannosidase II); J. Saraste, University of Bergen, Bergen, Norway (anti-rat p58); T. Rapoport, Harvard Medical School, Boston, MA and D. I. Meyer, University of California, Los Angeles, CA (anti-rat ribophorin I). Solutions of compactin and sodium mevalonate were prepared as previously described (Brown et al., 1978; Kita et al., 1980). Newborn calf lipoprotein-deficient serum ($d > 1.25$ g/ml) was prepared by ultracentrifugation (Goldstein et al., 1983).

### Plasmid Constructions

pGFP-SCAP encodes an Enhanced Green Fluorescent Protein/SCAP fusion protein (1539 amino acids), consisting of amino acids 1–239 of Enhanced Green Fluorescent Protein (Cormack et al., 1996), 25 amino acids encoded by a polylinker sequence, and amino acids 2–1276 of hamster SCAP (Hua et al., 1996a). Expression is driven by the CMV promoter/enhancer.

pVSVG-T7 encodes amino acids 1–512 of VSVG protein from the ts045 mutant strain of vesicular stomatitis virus (Gallione and Rose, 1985), followed by four novel amino acids (RTAA, codons generated by blunt-end ligation of filled-in BsiWI and NotI restriction sites), followed by two copies of the T7 tag (corresponding to the amino-terminal 11 amino acids of the T7 gene 10 protein). Codons 1–512 of VSVG/tsO45 were derived from pVSVG-GFP (Presley et al., 1997). Expression is driven by the CMV promoter/enhancer.

### Cell Culture

Chinese hamster ovary (CHO-K1) cells were grown in monolayer at 37°C in an atmosphere of 8%–9% $CO_2$ in medium A (a 1:1 mixture of Ham's F-12 medium and Dulbecco's modified Eagle medium containing 100 units/ml penicillin and 100 μg/ml streptomycin sulfate) supplemented with 5% (v/v) FCS. SRD-13A cells, a mutant subclone of CHO-7 cells (Rawson et al., 1999), were maintained in medium A supplemented with 5% FCS 5 μg/ml cholesterol, 1 mM sodium mevalonate, and 20 μM sodium oleate.

CHO/pGFP-SCAP cells were generated by transfection of SCAP-deficient SRD-13A cells with pGFP-SCAP, followed by selection in medium A supplemented with 5% newborn calf lipoprotein-deficient serum. pGFP-SCAP rescued the cholesterol auxotrophy of SRD-13A cells. Fluorescent colonies were cloned by limiting dilution. One clone that exhibited strong fluorescence, designated CHO/pGFP-SCAP, was expanded and used for experiments.

CHO/VSVG-T7 cells were generated by transfection of CHO-K1 cells with pVSVG-T7, followed by selection in medium A supplemented with 5% FCS and 0.7 mg/ml G418. Surviving colonies were isolated with cloning cylinders, expanded, and screened for expression of VSVG-T7 by immunoblotting. One positive clone, designated CHO/VSVG-T7 was cloned by dilution plating, expanded, and used for experiments.

### Buffers

The following buffers were used: PBS refers to phosphate-buffered saline, pH 7.4 (Cat. No. 21–031-CV, Mediatech, Herndon, VA). Buffer B contains PBS plus protease inhibitors (10 μg/ml leupeptin, 5 μg/ml pepstatin A, 2 μg/ml aprotinin, 25 μg/ml ALLN). Buffer C contains 10 mM Tris-HCl at pH 7.6, 100 mM NaCl, 1% (w/v) SDS plus protease inhibitors. Buffer D contains 150 mM Tris-HCl at pH 6.8, 15% SDS, 25% (v/v) glycerol, 0.02% (w/v) bromophenol blue, and 12.5% (v/v) 2-mercaptoethanol. Buffer E contains 50 mM HEPES-KOH at pH 7.2, 250 mM sorbitol, 70 mM KOAc, 5 mM potassium EGTA, 2.5 mM $Mg(OAc)_2$ plus protease inhibitors. Buffer F contains 10 mM HEPES-KOH at pH 7.2, 250 mM sorbitol, 10 mM KOAc, 1.5 mM $Mg(OAc)_2$ plus protease inhibitors.

### Time-Lapse Imaging

On day 0, cells were set up in glass-bottomed 35 mm dishes (Mat Tek Co., Ashland, MA) at a density of $3 \times 10^4$ cells/dish in medium A supplemented with 5% FCS. On day 2, cells were washed with PBS and refed 1 ml of medium A supplemented with 5% newborn calf lipoprotein-deficient serum and 0.2% ethanol. During the experiment, cells were maintained at 37°C in 5% $CO_2$ in an environmental chamber that encased the microscope stage. To start the experiment, 1 ml of medium A supplemented with 5% newborn calf lipoprotein-deficient serum and 2% (w/v) HPCD was added to the dish. The first image ($t = 0$ min) was recorded 4 min after addition of HPCD. GFP-SCAP was visualized with an inverted Leica TCS SP confocal microscope using a 488 nm laser and a Leica 63×/NA 1.3 PL APO oil immersion objective with a pinhole set to 1.5 times the Airy disk diameter. Digital images were captured every 2.5 min for 2.5 hr with no significant loss of signal. Images were edited using Adobe Photoshop 4.0, and the Quicktime movie was generated using Adobe Premier 5.1.

### Preparation of Rat Liver Cytosol

Male Sprague-Dawley rats (350–400 g) were housed in colony cages, maintained on a 12 hr light/12 hr dark cycle, and fed a Harlan Teklad 4% Mouse/Rat Diet 7001. At 3 hr into the dark cycle, the rats were anesthetized by halothane inhalation followed by an intraperitoneal injection of nembutal, after which their livers were perfused with 0.9% (w/v) NaCl through the portal vein at room temperature. The livers were excised and disrupted in 2 ml/g of ice-cold Buffer E supplemented with 1 mM dithiothreitol in a Polytron homogenizer followed by 10 strokes in a 50 ml Dounce homogenizer fitted with a teflon pestle. All subsequent steps were carried out at 4°C. Homogenates were centrifuged at $10^3 \times g$ for 10 min. Supernatants were sequentially centrifuged at $2 \times 10^4 \times g$ for 20 min, 186,000 × g for 1 hr, and 186,000 × g for 45 min. Following the 186,000 × g spins, care was taken to remove the fat layer before collecting the remaining aqueous supernatant. The final supernatant, designated as cytosol (24–33 mg protein/ml), was divided into multiple aliquots, snap-frozen in liquid nitrogen, and stored at −80°C. For experiments, tubes were thawed in a 37°C waterbath and placed on ice until use.

### Isolation of Microsomal Membranes from CHO Cells

Monolayers of CHO cells at 80%–90% confluency were scraped into 5 ml of ice-cold Buffer B, and pooled suspensions from duplicate 10 cm dishes were centrifuged at $10^3$ g for 5 min at 4°C. Each cell pellet was then resuspended in 1 ml of Buffer B, transferred to microcentrifuge tubes, and centrifuged again at $10^3$ g for 5 min at 4°C. Following aspiration of the supernatants, the tubes were snap-frozen in liquid nitrogen and (unless otherwise stated) stored at −80°C for up to one month until use. The tubes were thawed in a 37°C waterbath for 50 s and placed on ice. Each cell pellet was resuspended in 0.4 ml of Buffer F, passed through a 22-gauge needle 20 times, and centrifuged at $10^3$ g for 5 min at 4°C. The resulting supernatants were transferred to siliconized microcentrifuge tubes and centrifuged at $1.6 \times 10^4$ g for 3 min at 4°C in an Eppendorf model 5417C microcentrifuge. Subsequently, each pellet was resuspended in 0.5 ml of Buffer E, centrifuged again at $1.6 \times 10^4$ g for 3 min at 4°C, and resuspended in 60–100 μl of Buffer E to obtain microsomes for use in the in vitro vesicle-formation assay (described below). To determine the protein concentration, aliquots of the microsomal suspensions (5 μl) were added to 5 μl of a solution of 20% (w/v) of hexyl-β-D-glucopyranoside (Fanger, 1987) and assayed with Coomassie Plus Protein Assay Reagent (Pierce) according to the manufacturer's instructions using bovine serum albumin as a standard.

### In Vitro Vesicle-Formation Assay

The protocol used in this study was adapted from procedures described by the laboratories of Schekman (Rexach and Schekman, 1991) and Balch (Rowe et al., 1996). Each reaction contained, in a final volume of 80 μl, 50 mM HEPES-KOH at pH 7.2, 250 mM sorbitol, 70 mM KOAc, 5 mM potassium EGTA, 2.5 mM $Mg(OAc)_2$, 1.5 mM ATP, 0.5 mM GTP, 10 mM creatine phosphate, 4 units/ml of creatine kinase, protease inhibitors (described above under Buffers), 30–80 μg protein of CHO microsomes, and 600 μg of rat liver cytosol. Incubations were carried out in siliconized 1.5 ml microcentrifuge tubes for 15 min at 37°C (unless otherwise stated). Reactions were terminated by transfer of tubes to ice, followed by centrifugation at $1.6 \times 10^4$ g for 3 min at 4°C to obtain a medium-speed pellet (P16) and a medium-speed supernatant (S16). Aliquots (60 μl) of each S16 fraction were collected from the top of each sample and centrifuged again at $5.5 \times 10^4$ rpm at 4°C in a Beckman TLA100 rotor to obtain a high speed pellet (P100). P16 and P100 fractions were each resuspended in 60 μl of Buffer C, supplemented with 15 μl of Buffer D, and heated at 95°C for 5 min. Aliquots of the P16 (20 μl) and P100 fractions (75 μl) were subjected to 7% SDS-PAGE, transferred to nitrocellulose, and analyzed by immunoblotting. The P16 and P100 fractions are referred to as membranes and vesicles, respectively.

### Immunoblot Analysis

Gels were calibrated with molecular weight markers (Amersham or BioRad), and antibodies were used at the following concentrations: anti-SCAP IgG-R139, 5 μg/ml; anti-p58 serum, 1 μl/ml; anti-KDEL antibody (IgG fraction), 2 μg/ml; anti-ribophorin I serum, 0.2 μl/ml; anti-SREBP-1 IgG-2A4, 5 μg/ml; anti-SREBP-2 IgG-7D4, 5 μg/ml; anti-T7, 1 μg/ml; anti-HSV, 0.5 μg/ml; anti-rabbit IgG, 0.33 μl/ml; anti-mouse IgG, 0.2 μl/ml. Bound antibodies were visualized by chemiluminescence using the Supersignal Substrate System (Pierce) and exposed to Kodak X-Omat Blue XB-1 film (NEN) at room temperature for 1–120 s.

### Acknowledgments

We thank Amanda Hogle, Tammy Dinh, and Clinton Steffey for excellent technical assistance; Lisa Beatty, Jill Abadia, and Anna Fuller for invaluable help with tissue culture; Drs. Jennifer Lippincott-Schwartz, David Meyer, Kelley Moremen, Tom Rapoport, and Jaakko Saraste for generously providing antibodies and plasmids; and Dr. Richard Anderson for advice on confocal microscopy. This work was supported by grants from the National Institutes of Health (NIH) (HL-20948) and the Perot Family Foundation. P. J. E. is a recipient of an NIH Research Science Fellowship Grant (HL-09993).

Received March 29, 2000; revised June 21, 2000.

### References

Akusjarvi, G., Svensson, C., and Nygard, O. (1987). A mechanism by which adenovirus virus-associated $RNA_I$ controls translation in a transient expression assay. Mol. Cell. Biol. *7*, 549–551.

Beckers, C.J.M., Keller, D.S., and Balch, W.E. (1987). Semi-intact cells permeable to macromolecules: use in reconstitution of protein transport from the endoplasmic reticulum to the Golgi complex. Cell *50*, 523–534.

Bergmann, J.E. (1989). Using temperature-sensitive mutants of VSV to study membrane protein biogenesis. Meth. Cell Biol. *32*, 85–110.

Brown, M.S., and Goldstein, J.L. (1997). The SREBP pathway: regulation of cholesterol metabolism by proteolysis of a membrane-bound transcription factor. Cell *89*, 331–340.

Brown, M.S., and Goldstein, J.L. (1999). A proteolytic pathway that

controls the cholesterol content of membranes, cells, and blood. Proc. Natl. Acad. Sci. USA *96*, 11041–11048.

Brown, M.S., Faust, J.R., Goldstein, J.L., Kaneko, I., and Endo, A. (1978). Induction of 3-hydroxy-3-methylglutaryl coenzyme A reductase activity in human fibroblasts incubated with compactin (ML-236B), a competitive inhibitor of the reductase. J. Biol. Chem. *253*, 1121–1128.

Cormack, B.P., Valdivia, R.H., and Falkow, S. (1996). FACS-optimized mutants of the green fluorescent protein (GFP). Gene *173*, 33–38.

DeBose-Boyd, R.A., Brown, M.S., Li, W.-P., Nohturfft, A., Goldstein, J.L., and Espenshade, P.J. (1999). Transport-dependent proteolysis of SREBP: relocation of Site-1 protease from Golgi to ER obviates the need for SREBP transport to Golgi. Cell *99*, 703–712.

Duncan, E.A., Brown, M.S., Goldstein, J.L., and Sakai, J. (1997). Cleavage site for sterol-regulated protease localized to a Leu-Ser bond in lumenal loop of sterol regulatory element binding protein-2. J. Biol. Chem. *272*, 12778–12785.

Duncan, E.A., Davé, U.P., Sakai, J., Goldstein, J.L., and Brown, M.S. (1998). Second-site cleavage in sterol regulatory element-binding protein occurs at transmembrane junction as determined by cysteine panning. J. Biol. Chem. *273*, 17801–17809.

Edwards, P.A., and Ericsson, J. (1999). Sterols and isoprenoids: signaling molecules derived from the cholesterol biosynthetic pathway. Annu. Rev. Biochem. *68*, 157–185.

Ellgaard, L., Molinari, M., and Helenius, A. (1999). Setting the standards: quality control in the secretory pathway. Science *286*, 1882–1888.

Espenshade, P.J., Cheng, D., Goldstein, J.L., and Brown, M.S. (1999). Autocatalytic processing of Site-1 protease removes propeptide and permits cleavage of sterol regulatory element-binding proteins. J. Biol. Chem. *274*, 22795–22804.

Fanger, B.O. (1987). Adaptation of the Bradford protein assay to membrane-bound proteins by solubilizing in glucopyranoside detergents. Analyt. Biochem. *162*, 11–17.

Gallione, C.J., and Rose, J.K. (1985). A single amino acid substitution in a hydrophobic domain causes temperature-sensitive cell-surface transport of a mutant viral glycoprotein. J. Virol. *54*, 374–382.

Goldstein, J.L., Basu, S.K., and Brown, M.S. (1983). Receptor-mediated endocytosis of LDL in cultured cells. Meth. Enzymol. *98*, 241–260.

Hua, X., Nohturfft, A., Goldstein, J.L., and Brown, M.S. (1996a). Sterol resistance in CHO cells traced to point mutation in SREBP cleavage activating protein (SCAP). Cell *87*, 415–426.

Hua, X., Sakai, J., Brown, M.S., and Goldstein, J.L. (1996b). Regulated cleavage of sterol regulatory element binding proteins (SREBPs) requires sequences on both sides of the endoplasmic reticulum membrane. J. Biol. Chem. *271*, 10379–10384.

Kilsdonk, E.P.C., Yancey, P.G., Stoudt, G.W., Bangerter, F.W., Johnson, W.J., Phillips, M.C., and Rothblat, G.H. (1995). Cellular cholesterol efflux mediated by cyclodextrins. J. Biol. Chem. *270*, 17250–17256.

Kita, T., Brown, M.S., and Goldstein, J.L. (1980). Feedback regulation of 3-hydroxy-3-methylglutaryl coenzyme A reductase in livers of mice treated with mevinolin, a competitive inhibitor of the reductase. J. Clin. Invest. *66*, 1094-1100.

Klumperman, J., Schweizer, A., Clausen, H., Tang, B.L., Hong, W., Oorschot, V., and Hauri, H.-P. (1998). The recycling pathway of protein ERGIC-53 and dynamics of the ER-Golgi intermediate compartment. J. Cell Sci. *111*, 3411–3425.

Krieger, M., Goldstein, J.L., and Brown, M.S. (1978). Receptor-mediated uptake of low density lipoprotein reconstituted with 25-hydroxycholesteryl oleate suppresses 3-hydroxy-3-methylglutaryl-coenzyme A reductase and inhibits growth of human fibroblasts. Proc. Natl. Acad. Sci. USA *75*, 5052–5056.

Nohturfft, A., Brown, M.S., and Goldstein, J.L. (1998a). Topology of SREBP cleavage-activating protein, a polytopic membrane protein with a sterol-sensing domain. J. Biol. Chem. *273*, 17243–17250.

Nohturfft, A., Brown, M.S., and Goldstein, J.L. (1998b). Sterols regulate processing of carbohydrate chains of wild-type SREBP cleavage-activating protein (SCAP), but not sterol-resistant mutants Y298C or D443N. Proc. Natl. Acad. Sci. USA *95*, 12848–12853.

Nohturfft, A., DeBose-Boyd, R.A., Scheek, S., Goldstein, J.L., and Brown, M.S. (1999). Sterols regulate cycling of SREBP cleavage-activating protein (SCAP) between endoplasmic reticulum and Golgi. Proc. Natl. Acad. Sci. USA *96*, 11235–11240.

Palade, G.E. (1975). Intracellular aspects of the process of protein secretion. Science *189*, 347–358.

Presley, J.F., Cole, N.B., Schroer, T.A., Hirschberg, K., Zaal, K.J.M., and Lippincott-Schwartz, J. (1997). ER-to-Golgi transport visualized in living cells. Nature *389*, 81–85.

Rawson, R.B., Zelenski, N.G., Nijhawan, D., Ye, J., Sakai, J., Hasan, M.T., Chang, T.-Y., Brown, M.S., and Goldstein, J.L. (1997). Complementation cloning of *S2P*, a gene encoding a putative metalloprotease required for intramembrane cleavage of SREBPs. Molecular Cell *1*, 47–57.

Rawson, R.B., DeBose-Boyd, R., Goldstein, J.L., and Brown, M.S. (1999). Failure to cleave sterol regulatory element-binding proteins (SREBPs) causes cholesterol auxotrophy in Chinese hamster ovary cells with genetic absence of SREBP cleavage-activating protein. J. Biol. Chem. *274*, 28549–28556.

Rexach, M.F., and Schekman, R.W. (1991). Distinct biochemical requirements for the budding, targeting, and fusion of ER-derived transport vesicles. J. Cell Biol. *114*, 219–229.

Rowe, T., Aridor, M., McCaffery, J.M., Plutner, H., Nuoffer, C., and Balch, W.E. (1996). COPII vesicles derived from mammalian endoplasmic reticulum microsomes recruit COPI. J. Cell Biol. *135*, 895–911.

Sakai, J., Nohturfft, A., Cheng, D., Ho, Y.K., Brown, M.S., and Goldstein, J.L. (1997). Identification of complexes between the COOH-terminal domains of sterol regulatory element binding proteins (SREBPs) and SREBP cleavage-activating protein (SCAP). J. Biol. Chem. *272*, 20213–20221.

Sakai, J., Nohturfft, A., Goldstein, J.L., and Brown, M.S. (1998). Cleavage of sterol regulatory element binding proteins (SREBPs) at site-1 requires interaction with SREBP cleavage-activating protein. Evidence from *in vivo* competition studies. J. Biol. Chem. *273*, 5785–5793.

Sato, R., Yang, J., Wang, X., Evans, M.J., Ho, Y.K., Goldstein, J.L., and Brown, M.S. (1994). Assignment of the membrane attachment, DNA binding, and transcriptional activation domains of sterol regulatory element binding protein-1 (SREBP-1). J. Biol. Chem. *269*, 17267–17273.

Springer, S., Spang, A., and Schekman, R. (1999). A primer on vesicle budding. Cell *97*, 145–148.

Wang, X., Sato, R., Brown, M.S., Hua, X., and Goldstein, J.L. (1994). SREBP-1, a membrane-bound transcription factor released by sterol-regulated proteolysis. Cell *77*, 53–62.

Yang, J., Brown, M.S., Ho, Y.K., and Goldstein, J.L. (1995). Three different rearrangements in a single intron truncate SREBP-2 and produce sterol-resistant phenotype in three cell lines. J. Biol. Chem. *270*, 12152–12161.